2022 IEEE International Conference on Robotics and Automation (ICRA)
May 23-27, 2022. Philadelphia, PA, USA

KHAOS: a Kinematic Human Aware Optimization-based System for Reactive Planning of Flying-Coworker

Jérôme Truc[1], Phani-Teja Singamaneni[1], Daniel Sidobre[1], Serena Ivaldi[2] and Rachid Alami[1]

***Abstract*— The use of drones in human-populated areas is increasing day by day. Such robots flying in close proximity to humans and potentially interacting with them, as in object handover or delivery, need to carefully plan their navigation considering the presence of humans. We propose a human-aware 3D reactive planner based on stochastic optimization for drone navigation. Besides considering the kinematics constraints of the drone, we propose two criteria to produce socially acceptable trajectories. The first, called discomfort, considers the unease caused to the humans spatially close to fast-moving drones. The second, called visibility, promotes the drone's visibility for humans. We demonstrate the planner's performance and adaptability in various simulated experiments.**

I. Introduction

Drones use is increasing in our society, with new applications in human-populated areas which go beyond leisure and visual inspection. With increased payload and interaction capabilities, they are now considered for object delivery and collaboration with workers in civil and industrial applications. Safety is paramount. However, navigation and interaction in close proximity to humans call for the consideration of some specific social skills, such as producing legible and acceptable motions [1], [2], [3].

In this paper, we address navigation planning in the scenario of the "Flying Co-Worker"[3]: a multi-rotor drone that collaborates with workers to fetch small objects. The robot must fly in a human-populated area, where only a handful of human workers may be "aware" of the robot's current task and mission, and a fraction of them may be involved in the physical interaction (e.g., object delivery): the robot must assume that most humans are "observers", i.e., they ignore its current mission and are not involved with it. In such conditions, the drone needs to carefully plan its 3D motion in a reactive way to navigate and act safely in close proximity to humans. Beyond safety, the drone should aim at exhibiting navigation strategies that are, as much as possible, socially aware: for example, it should avoid fast movements close or toward humans which could scare the observers; it should maximize its visibility for workers, especially when engaging in an interaction.

[1] LAAS-CNRS, Université de Toulouse, CNRS, UPS, Toulouse, France `firstname.lastname@laas.fr`
[2] Inria, Université de Lorraine, CNRS, F-54000.
[3] This work was partially supported by the French National Research Agency (ANR) (project Flying Co-Worker, `https://www.laas.fr/projects/flying_coworker`, grant ANR-18-CE33-0001), the European Commission (AnDy, GA. n. 731540; CHIST-ERA - HEAP) and the Artificial and Natural Intelligence Toulouse Institute - Institut 3iA (ANITI) under grant agreement No: ANR-19-PI3A-0004.

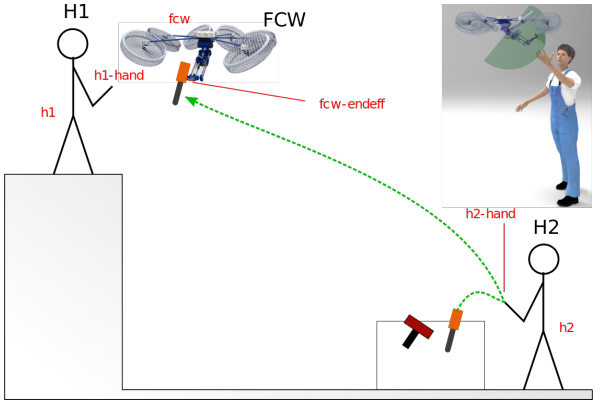

Fig. 1: Conceptual representation of the Flying Coworker with the 3DoF arm in a handover operation with a human worker. Human-2 (H2) has the tool required by Human-1 (H1) and the drone (FCW - Flying Coworker) carries the tool from H2 to H1. The picture on top right corner is the 3D visualisation of this handover by H2.

We propose a Kinematic Human-Aware Optimization System (KHAOS) for reactive navigation planning which addresses the requirements mentioned above by synthesizing trajectories in the 3D space satisfying the kinematic constraints of the drone and ensuring the visibility and ease of the humans present in the environment. The human-aware behavior is realized by proposing a visibility cost and a novel discomfort cost and including these along with the kinematic constraints into a stochastic optimization process inspired by the STOMP algorithm [4]. These measures for the social navigation of the drones, together with the new reactive planning system, KHAOS, are the main contributions of this paper. In this work, we consider only multi-rotor drones, and throughout this paper, the term drone always refers to a multi-rotor drone.

The organization of the rest of the paper is as follows. We briefly review related work in section II, and then we describe in section III the different costs and constraints used by our trajectory optimizer after giving some details on its operation. We show in section IV the behavior of the obtained reactive planner through several illustrative examples. Finally, section V is dedicated to a discussion about the planner performance and potential improvements, followed by conclusions in section VI.

II. Related Work

Human-aware robot navigation needs to consider additional constraints on the plan as well as the motion of the robot [1] to navigate safely around the humans. Most of the

2022 IEEE International Conference on Robotics and Automation (ICRA) | 978-1-7281-9681-7/22/$31.00 ©2022 IEEE | DOI: 10.1109/ICRA46639.2022.9811803

human-aware navigation planners mainly use only the so-called proxemics [1], [2] criteria. The work of Ferrer. et al [5] and, Repiso et. al [6] uses a social force model (SFM) based controller to navigate in the crowd and to accompany humans. Truong et. al [7] extended this to human-object and human-group interactions by proposing the proactive social motion model. Inspired by these, Garell et. al [8] proposes an Aerial Social Force Model (ASFM), a 3D SFM, that allows the drones to safely accompany humans. Some recent works in ground robot navigation use Graph Convolutional Networks [9] and reinforcement learning [10] to learn acceptable navigation behaviors for the robot. A recent contribution uses optimization to produce more legible robot trajectories along with modality shifting to address multi context navigation [11]. In case of drone navigation, the recent work of Garell et. al [12] focuses on using neural networks to learn the non-linear ASFM to address the problem of human accompaniment. Unlike the ASFM which focuses on a reactive controller, we present a reactive planning approach in this paper inspired by the STOMP algorithm [4] which is highly flexible and can be adapted to various situations.

When the robot needs to approach a human for interaction, new motion criteria such as approach the user from the front [13], [14] and at a reduced speed, [15] are introduced. The noise and the wind generated by the propellers of drones cause significant additional annoyance for people as mentioned in [16]. A user study carried out by Duncan et al. [17] evaluating the approach distance and height of the drone towards a human concluded that the human-human proxemics might not be directly transferable to human-aerial robot interactions. Yeh et al. [18] also performed a user study for evaluating proxemics in human-drone interaction and showed that the personal space of the humans varied based on social cues, like greeting and the design of the drone. A more recent work by Jensen et al. [19] studied the drone's interaction distance with a human to signal its presence and concluded that humans feel acknowledged between $2\,\mathrm{m}$ to $4\,\mathrm{m}$. At this point, one could also wonder what is the best angle of approach to interact with a human as studied for a mobile robot by Koay et al. [14] who show a preference of the users for a frontal approach, in the visual field of the human. In our work, the field of view of humans, the effort to get the drone visible, and the discomfort caused to the humans by the drone's motion are considered to propose a plan that is less disturbing for the interacting humans (professionals) while avoiding the observers in a safe and friendly way.

Pertinent communication of intentions by the robot can also improve legibility [20] and safety. These intentions can be communicated by a more 'readable' trajectory of the robot as discussed by Dragan et al. [20] or with some gestures [21] or through gaze [22], [23]. A recent work by Bevins and Duncan [24] studies the human perception of different drone paths and their responses to them. They generated several types of paths and based on a 3 phase user study, they proposed some guidelines on the design of robot paths for communication. Works by Kruse et. al [25] and Sisbot et al. [26] studied the effect of directional costs and visibility to produce more legible paths for robot navigation. The approach presented in [27], [28] proposed proactive trajectory planning for co-operative human-robot navigation and introduced *time_to_collision*, a cost predicting a future collision with a human and pushing the robot to act earlier and show its intention to the human. The *discomfort_cost* proposed in this paper is inspired by this. Similar behavior was applied to the case of the drone in [29], showing this anticipation effect where the drone takes into account the perception of the human. The results of the study by Szafir et al. [30] show the importance of taking into account the phases of acceleration and deceleration of the drone and therefore, its kinematics to improve their social integration in an environment where they collaborate with humans.

III. Human-Aware Reactive Trajectory Planner

We need a reactive planner which can perform well in a 3D environment that is not too sensitive to different local minima. We propose an approach inspired by the STOMP algorithm [4] which allows great flexibility due to its stochastic nature. The optimization takes as input a list of points forming an original path whose ends are the start position and the desired goal. From this original path, it generates K noisy trajectories exploring the surrounding space and calculates the associated costs. These K trajectories are then analyzed using different costs applied at each timestep or waypoint to sort the most interesting configurations and finally generate an optimized trajectory. Below, we define the various costs that we use to help the optimizer generate safe and comfortable trajectories for humans in the scene. Then, we adapt the optimization algorithm to take into account not only the kinematic constraints of the robot but also the constraints imposed to respect human comfort.

A. Human-Aware Costs

1) Discomfort: To represent the discomfort caused to one or more humans when a drone moves in the environment, we consider a cost based on the relative speed and distance between the drone and humans present. Indeed, we want to translate the fact that a drone moving fast and close to a human is much less comfortable than a distant slow drone. In addition, if the drone is forced in one way or another to pass close to a human, it must adapt its speed by reducing it to limit the discomfort generated to this human, or even stop if it has reached a certain threshold. The *time_to_collision* cost presented in [27] is the first part of the answer, but we want information on this cost even when the velocity vector of the drone is not oriented towards the human. Therefore, we formulate the *discomfort_cost* as:

$$C_{dis} = \frac{\|\overrightarrow{V_{rob}} - \overrightarrow{V_{hum}}\|}{Dist_{rob-hum}} + \frac{\alpha_{proximity}}{Dist^2_{rob-hum}} \tag{1}$$

where $\|\overrightarrow{V_{rob}} - \overrightarrow{V_{hum}}\|$ and $Dist_{rob-hum}$ are respectively the relative speed and distance between the drone and the human. The second term of Eq. (1) describes the cost associated with

the proximity of the drone to the human whose influence can be adjusted using the scaling factor $\alpha_{proximity}$.

2) Visibility and effort to see: The visibility criterion presented in [26] uses a 2D grid. Since a drone can move in three dimensions, we need to extend the model to a 3D grid. The 3D grid centered at the origin of the human visual field gives the visibility cost, C_{vis}, for each cell which is computed as follows:

- All cells contained in a cone of pan and tilt angles respectively equal to $2 * |\alpha|$ and $2 * |\alpha'|$ (blue zone in Fig. 2a and Fig. 2b) located in front of the human have the same cost value. This value is relatively low (= 1) representing a relatively free zone and corresponding to the preferential approach zone according to [14].
- Angles increase clockwise as $|\beta| = \pi - |\alpha|$ and $|\phi| = \pi - |\alpha|$. Cells in the zone starting at $|\alpha_{max}|$ (respectively $|\alpha'_{max}|$) and ending at $|\beta_{max}|$ (respectively $|\phi_{max}|$) have a cost proportional to $|\alpha| + |\beta|$ (respectively $|\alpha'| + |\phi|$). This makes it possible to reconcile the approach zones in the visual field which are less comfortable than the frontal zone and the zones which are not in the visual field of the human that require an effort to turn around.
- Zones hidden by obstacles, out of the visual field and beyond a threshold distance ($4\,\mathrm{m}$) correspond to a zero cost value.

As depicted in Fig. 2, we can see the orientation of the human gaze represented by the red arrow. Directly in front of human is represented in dark blue, the zone of low cost, and then there is a gradual increase of the cost more and more towards the rear corresponding to more and more reddish colors.

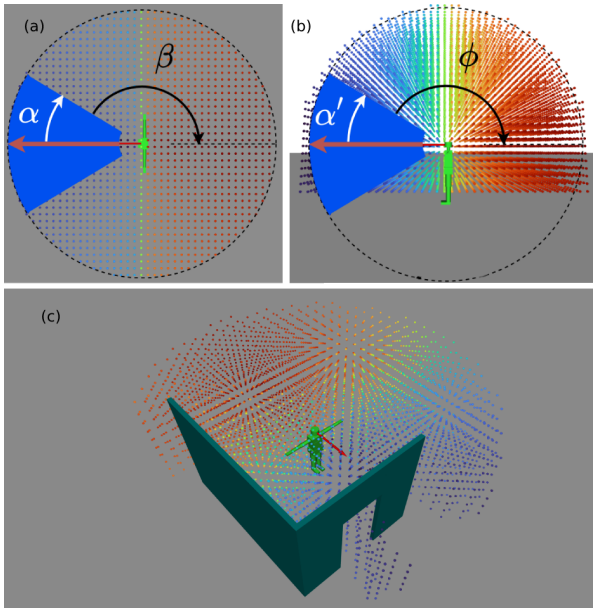

Fig. 2: Visibility cost : a) (resp. b) Cutaway top (resp. side) view showing the 3D simulation rendering of the change in visibility cost as a function of the panoramic (resp. tilt) angle. c) 3D view showing the consideration of obstacles. The human gaze direction is represented by a red arrow. Red colored cells correspond to high cost while blue colors correspond to low cost.

Algorithm 1: Constrained velocity computation

Given;
- Drone kinematics constraints: v_{max}, a_{max}, dec_{max}
- *discomfort_constraint*: DCF_{max}

for *each noisy smooth trajectory* **do**
  for *each 3D position of the drone* **do**
    Compute kinematic velocity of the drone v_{kin};
    Compute discomfort cost C_{dis} with v_{kin};
    if $C_{dis} < DCF_{max}$ **then**
      $v_{choice} = v_{kin}$;
    else
      $v_{choice} = (DCF_{max} - \frac{\alpha_{proximity}}{Dist^2_{hum-rob}}) * Dist_{hum-rob}$;
    end
    $v_{drone} = min(v_{max}, v_{choice})$
  end
end

B. Kinematic constraints

The driving idea behind our approach is to take into account the kinematics of the drone while respecting human comfort by taking as a reference the *discomfort_cost* defined above. The particularity of the STOMP algorithm on which we based the optimization part of our approach is the generation and comparison of K noisy trajectories aiming to explore space in a stochastic manner. Starting from this principle, we propose in Algorithm 1 to constrain these K generated trajectories by considering the kinematic constraints of the drone such as its maximum speed v_{max}, acceleration a_{max} and deceleration dec_{max}. To this, we add an additional constraint linked to the cost of discomfort by setting a value DCF_{max}, which cannot be exceeded and named as *discomfort_constraint* in this paper. Thus for each point of the trajectory generated randomly, we calculate the maximum speed v_{kin} that the drone can reach considering its kinematics limits and, if for this position and speed, the C_{dis} exceeds *discomfort_constraint* limit DCF_{max}, then the *discomfort_constraint* predominates and limits the speed below the maximum speed that it is possible to achieve. Conversely, if for a given position, the drone can move at its maximum speed and it is not inconvenient for humans, then it will limit its speed to its maximum kinematic limits.

C. Local cost and Trajectory cost

Similar to the STOMP algorithm [4], we calculate the cost for each timestep or waypoint at the local level and an overall trajectory cost. The local cost function is defined as the sum of the visibility cost, C_{vis}, discomfort cost, C_{dis} and obstacle cost, $C_{obstacles}$, which pushes the waypoints away from the obstacles whenever possible without violating the social constraints. For the calculation of the trajectory cost, we define a time cost, C_{time}, which is the combination of the path length and sum of the velocities at each timestep.

Finally, the total cost of trajectory is defined as follows:

$$C_{total} = \sum_{i=1}^{N} C_{vis} + C_{time} \tag{2}$$

where, N is the number of waypoints, $C_{time} = \alpha_{time} * \frac{L}{V}$, L is the length of the trajectory, V is the sum of the magnitude of the velocity at each waypoint and α_{time} is a constant. The optimization converges when the change in the total cost of the trajectory is below the chosen threshold.

IV. Evaluation in Simulated Experiments

In this section, we first give more details about the implementation of KHAOS. Then, we present the results and analysis of the proposed trajectory planner in five different scenarios that show the robustness of our system. By default, the results presented in this section correspond to a maximum speed of the drone of $1\,\mathrm{m\,s^{-1}}$. Likewise, the maximum acceleration and deceleration are fixed at around $1\,\mathrm{m\,s^{-2}}$. The study of the influence of the orientation of the drone is not taken into account as a social constraint here, and the orientation of the drone is the same as its velocity vector.

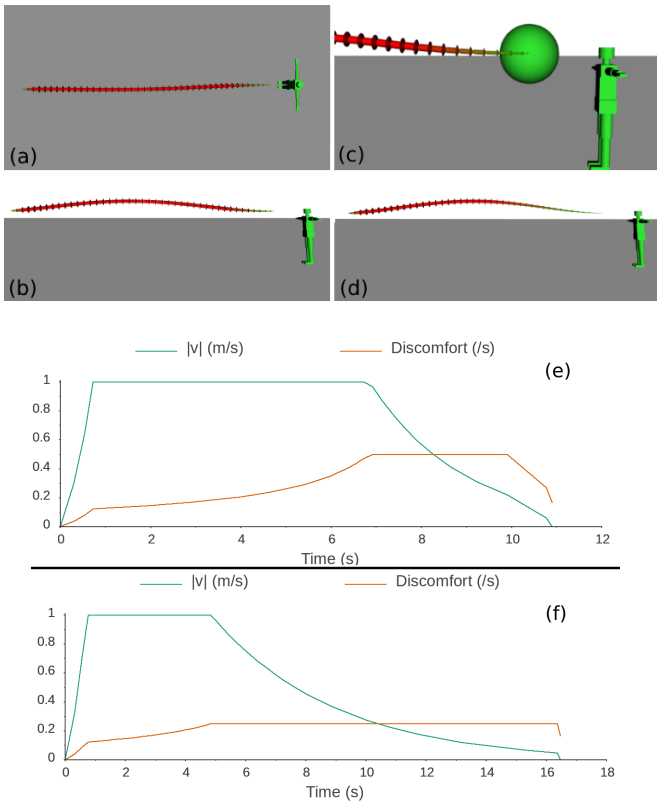

Fig. 3: Frontal approach with a *discomfort_constraint* of 0.5: a) Top view b) Side view c) Side view with a zoom at the top showing the drone's size represented by a sphere of $0.9\,\mathrm{m}$ e) Drone speed and *discomfort_cost* as a function of time. Frontal approach with a *discomfort_constraint* of 0.25: d) Side view f) Drone speed and *discomfort_cost* as a function of time.

A. Setup

The simulation results presented here use the MoveIt [31] collision scene in which the model of a human is imported. This model is composed of simple primitives such as spheres, cylinders and boxes. The drone is considered as a $0.9\,\mathrm{m}$ diameter sphere that can be configurable and is not shown in the images to improve readability (except in Fig 3b), showing only its trajectories. Obstacles present in some results are added in the same way. We can thus manage the numerous collision tests necessary for the optimizer and the computation of 3D grids directly with MoveIt [31] or else externally using FCL [32].

B. Frontal approach

In this scenario, as shown in Fig. 3, the drone starts at a distance of $9\,\mathrm{m}$ from the human and approaches him at a very close distance of $0.5\,\mathrm{m}$ and at a height of $1.5\,\mathrm{m}$. This interaction distance is very small and close to the human's head, which can be considered a very uncomfortable situation for him. A *discomfort_constraint* equal to 0.5 is chosen and it can be imagined as the maximum speed of $1\,\mathrm{m\,s^{-1}}$ for the drone at a distance of $2\,\mathrm{m}$ from the human. We represent the trajectory by drawing each of its segments with an arrow whose color depends on the average speed. The more the color tends towards red, the higher the speed and the more the color tends towards green, the slower the speed. From this representation, we can visually see the phases of acceleration and deceleration of the drone. As the approach is frontal, the cost of the human visual field does not influence and does not distort the trajectory. In our implementation, we favor positions far from obstacles, and that explains the slight deformation of the trajectory towards the opposite direction of the ground, which is considered as an obstacle.

We can find these phases in Fig. 3e representing the speed of the drone as well as the *discomfort_cost* along the trajectory. First of all, the drone accelerates in accordance with its kinematic limits until it reaches its maximum speed of $1\,\mathrm{m\,s^{-1}}$. Gradually approaching the human, the *discomfort_cost* increases until it reaches the *discomfort_constraint* of 0.5 that we have set. Once this maximum value is reached, the optimizer will regulate the speed and start to decelerate so as not to violate either the *discomfort_constraint* or the kinematic constraints of the drone. Let us now consider the same trajectory but this time we fixed the *discomfort_constraint* at 0.25. In Fig. 3f, we find the same acceleration phase as before. On the other hand, the *discomfort_constraint* is reached more quickly which pushes the drone to slow down approximately $2\,\mathrm{s}$ earlier, allowing the drone to signal to the human its intention to slow down in his/her presence. In addition, the deceleration phase is much longer by around $3\,\mathrm{s}$, which gives time to the human to adapt better to the presence of the drone.

C. Two Humans

Until now, the trajectories generated by KHAOS are not subject to constraints linked to the environment except the human himself. Now let's study Fig. 4, a situation where the drone firstly navigates in a corridor and crosses a human represented in blue on its way, then continues by approaching a second human in green from the back to finish at a position

where it can exchange an object with him. For this, we added 2 walls 3 m high, positioned so that there is sufficient space for the drone to navigate to the human's right in the corridor. A ceiling is added to the corridor to force the drone through it instead of going around it. Each human has his own visibility grid computed. For a given position in the optimization process, we consider the maximum value of the *visibility_cost* and *discomfort_constraint* between the different humans in the scene.

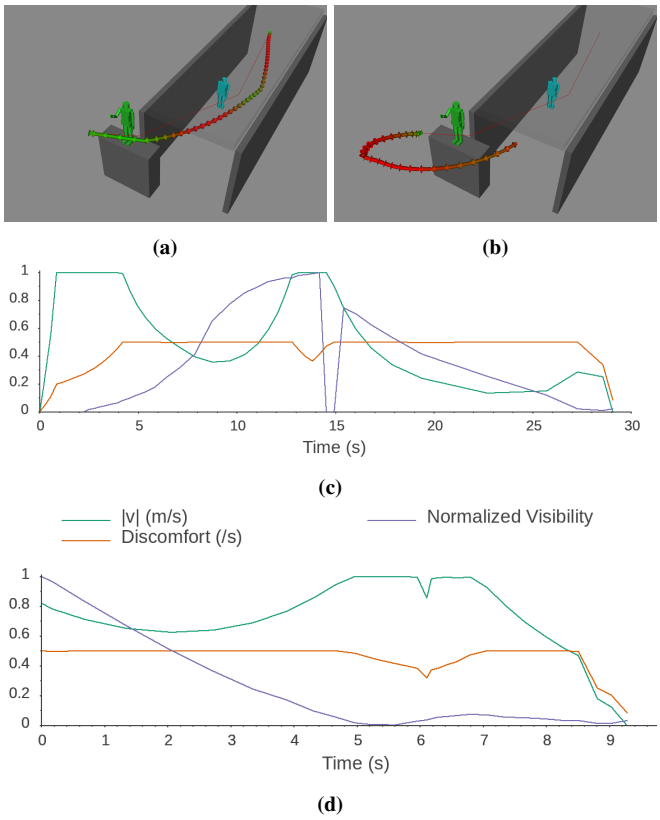

Fig. 4: Trajectory execution in a two-humans scenario for a *discomfort_constraint* of 0.5. a) First iteration, the robot starts by navigating in the corridor b) A few iterations later, after having passed the blue human in the corridor c) (resp. d) speed magnitude, *discomfort_cost* and *visibility_cost* as a function of time corresponding to the trajectory from (a) (resp b: Time origin corresponds to the beginning of the re-planned trajectory).

In this situation, the corridor walls do not allow the optimizer to generate trajectories that deviate greatly from the human in blue. Despite the constraints induced by the walls, the speed is close to the maximum speed along the trajectory except for the points closest to the blue human. Here, the points of the trajectory are spatially blocked by the wall, and therefore the *discomfort_cost* takes over by limiting the speed. This is what we observe in Fig. 4c between 4 and 13 s when the speed is limited by the *discomfort_constraint*. At the same time, we can observe that the *visibility_cost* greatly increases because the drone goes more and more towards the back of the blue human and can't pass far from him until it comes out of the grid at approximately 14.5 s and *visibility_cost* drop to 0.

Once the drone has passed the human in blue, it finds itself behind the back of another human represented in green. Here, the influence of his *visibility_cost* becomes predominant compared to that of the human in blue. The trajectory greatly deviates as shown in Fig. 4b and this shows how our planner ensures to limit the effort necessary for the human to turn his head, and thus have the drone in his field of view while respecting the *discomfort_constraint*. Fig. 4d shows that the drone moves away from the human by adapting its speed and reduces the effort required to see it specifically at the end when it is in close proximity to the human.

In the situation where the drone disengages from the human after handover (Fig. 5a), the shape of the trajectory is similar to the approach from the back. It first prioritizes the positions in front of the human to move away and go around the human. It accelerates smoothly, as shown in Fig. 5b until the first 2 s, limited by the *discomfort_cost*, and then adapts its speed in agreement with other constraints.

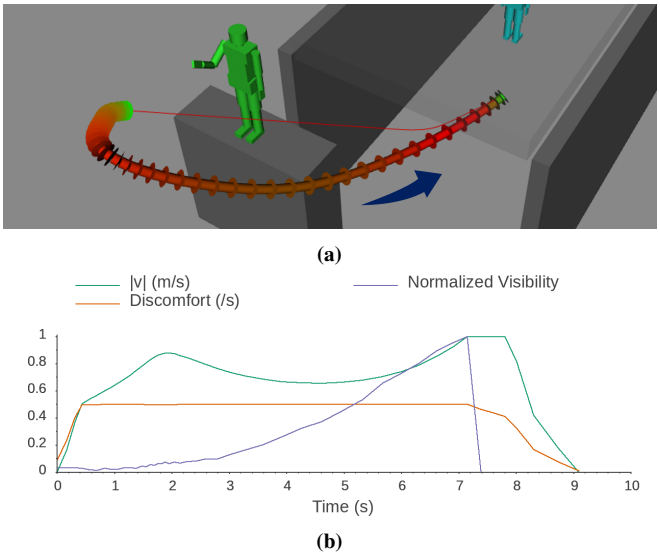

Fig. 5: Drone disengagement from the human and motion toward the corridor with a *discomfort_constraint* of 0.5. a) Shape of the trajectory b) speed magnitude, *discomfort_constraint* and *visibility_cost* as a function of time. Blue arrow indicates the direction of the trajectory.

D. Planner reactivity

In order to illustrate the reactivity of our planner, we use the corridor scenario like the one above. Fig. 6a shows the trajectory deformation with the *discomfort_constraint* fixed at 0.25. We then move the human to his right towards the wall and reduce the drone's initial passage space, as shown in Fig. 6b. We observe in Fig. 6b that the planner reacts immediately by deviating the path and reducing the speed (Fig. 6d) when close to the human.

E. Highly constrained environment

We want to show the KHAOS's ability to adapt and find solutions even in very constrained environments. For that, we take the previous corridor scene and add an obstacle that can be compared to a counter in order to restrict the

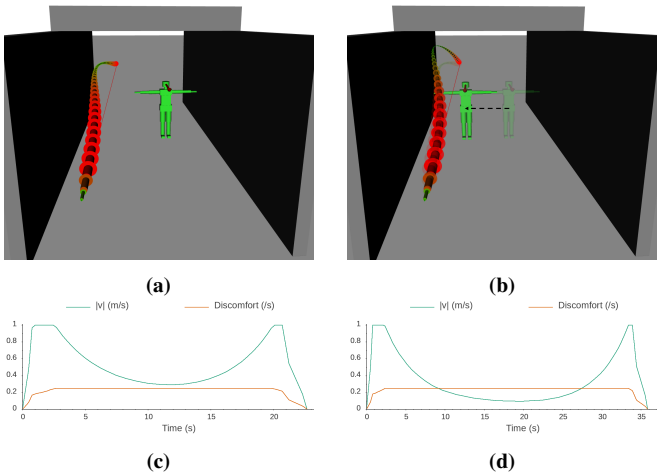

Fig. 6: Planner reactivity after moving the human to his right for a *discomfort_constraint* of 0.25. On the left: First iteration (a) with corresponding drone's speed magnitude and *discomfort_cost* as a function of time (c). On the right: Next iteration just after moving the human on his right reducing the passage to the drone (b) with its corresponding speed magnitude and *discomfort_cost* as a function of time (d).

possibilities of the passage of the drone through the place where the human is located. It is placed on the ground and prevents access to the drone from the area below the human's right arm. The space between the ceiling and the human's head is sufficient for the drone to pass, but in this case, the trajectory would be very uncomfortable for the human or even dangerous. We deliberately challenge KHAOS by choosing an original path passing through the area below the human's left arm represented by the red line in Fig. 7. Flying

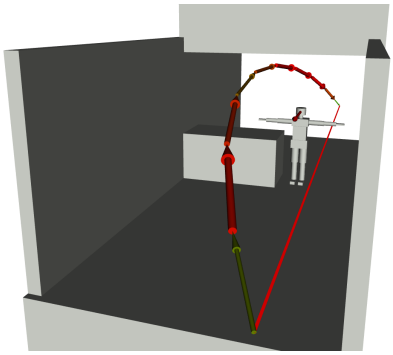

Fig. 7: Drone's trajectory along the constrained corridor with a *discomfort_constraint* of 0.5.

in this area would push it to pass very close to the human body, which would be very uncomfortable. If the drone had no other choice, the optimizer would be able to generate a trajectory where the drone would go at a very slow speed as it passes close to the human body. In the case presented here, the optimizer chooses a trajectory far from the human and on the opposite side by changing the homotopy class. We, therefore, can say that the trajectories generated by the optimizer are not deformed just locally but by exploring the surrounding space to find more suitable solutions. This trajectory is not only more comfortable for the human but also allows the drone to reach its goal more quickly.

V. DISCUSSION

The trajectory is generated and refreshed at a frequency between 5-10Hz on a standard computer (1.9 GHz Intel i7 CPU, 32 GB of memory): with such a performance, our reactive planner can be used in real-time in real robot experiments. Trajectories used in our experiments are generated from an original path corresponding to a straight line to simplify reading except for the two humans scenario. Indeed, in our case, we must be attentive not only to the shape of the trajectories but also to the adaptation of the speed. The noise generated by a multi-rotor drone is a function of its speed and/or acceleration. Moreover, the acoustic intensity decreases proportionally to the inverse of the square of the distance. We can therefore consider the *discomfort_constraint* described in this paper provides to reducing this nuisance as well. The physical model used for the calculation of the speeds of the drone by considering the *discomfort_constraint* can be improved. At some parts of the trajectory the speed is not derivable, but most of the time, the system produces a smooth motion compatible with human interaction. To improve it, we can combine it with the bounded jerk model techniques [33] that could produce smoother and better velocity profiles.

VI. CONCLUSION

We have presented an algorithm called KHAOS for the generation of reactive human-aware trajectories in 3D and taking into account the kinematic constraints of a drone, the potential discomfort caused by the robot's fast motion close to the human as well as its visibility, and the consideration of human effort to see it. We proposed a discomfort cost considering the relative distances and speeds between a drone and a human. We have shown how the drone adapts its behavior in several situations and have discussed the capabilities of the proposed planner. The reactivity of this planner in these different scenarios is highlighted in the attached video. In future work, we plan to improve the planner by adding the management of drone orientation and using it effectively on a real drone. We also plan to improve the behavior of the drone by working on the smoothing of speeds and accelerations. On the human-aware level, we want to go more in-depth by studying how to adapt the trajectories by integrating the handover phase [34] as well as the control of the manipulator's arm [35], which requires being very close to the human. We aim at a coordinated arm movement which can, for example, start reaching to exchange an object while the navigation phase is not yet over, which requires testing deformable configuration spaces for the drone. Finally, we will carry out a user study to tune the parameters of the social constraints and to assess whether the trajectories generated by KHAOS are socially acceptable and to which extent they can be improved based on users feedback from experiments with the real robot.

REFERENCES

[1] T. Kruse, A. K. Pandey, R. Alami, and A. Kirsch, "Human-aware robot navigation: A survey," *Robotics and Autonomous Systems*, 2013.

[2] J. Rios-Martinez, A. Spalanzani, and C. Laugier, "From proxemics theory to socially-aware navigation: A survey," *International Journal of Social Robotics*, 2015.

[3] C. Mavrogiannis, F. Baldini, A. Wang, D. Zhao, P. Trautman, A. Steinfeld, and J. Oh, "Core challenges of social robot navigation: A survey," 2021.

[4] M. Kalakrishnan, S. Chitta, E. Theodorou, P. Pastor, and S. Schaal, "STOMP: Stochastic trajectory optimization for motion planning," in *2011 IEEE International Conference on Robotics and Automation*.

[5] G. Ferrer, A. Garrell, and A. Sanfeliu, "Social-aware robot navigation in urban environments," in *2013 European Conference on Mobile Robots*, IEEE.

[6] E. Repiso, G. Ferrer, and A. Sanfeliu, "On-line adaptive side-by-side human robot companion in dynamic urban environments," in *2017 IEEE/RSJ International Conference on Intelligent Robots and Systems*.

[7] X.-T. Truong and T. D. Ngo, "Toward socially aware robot navigation in dynamic and crowded environments: A proactive social motion model," *IEEE Transactions on Automation Science and Engineering*, 2017.

[8] A. Garrell, L. Garza-Elizondo, M. Villamizar, F. Herrero, and A. Sanfeliu, "Aerial social force model: A new framework to accompany people using autonomous flying robots," in *2017 IEEE/RSJ International Conference on Intelligent Robots and Systems (IROS)*.

[9] C. Chen, S. Hu, P. Nikdel, G. Mori, and M. Savva, "Relational graph learning for crowd navigation," *arXiv preprint arXiv:1909.13165*, 2019.

[10] R. Guldenring, M. Görner, N. Hendrich, N. J. Jacobsen, and J. Zhang, "Learning local planners for human-aware navigation in indoor environments," in *2020 IEEE/RSJ International Conference on Intelligent Robots and Systems (IROS)*.

[11] P. T. Singamaneni, A. Favier, and R. Alami, "Human-aware navigation planner for diverse human-robot contexts," in *IEEE/RSJ International Conference on Intelligent Robots and Systems (IROS)*, 2021.

[12] A. Garrell Zulueta, C. Coll Gomilla, R. Alquézar Mancho, and A. Sanfeliu Cortés, "Teaching a drone to accompany a person from demonstrations using non-linear asfm," in *2019 IEEE/RSJ International Conference on Intelligent Robots and Systems (IROS)*.

[13] K. Dautenhahn, M. Walters, S. Woods, K. L. Koay, C. L. Nehaniv, A. Sisbot, R. Alami, and T. Siméon, "How may i serve you? a robot companion approaching a seated person in a helping context," in *Proceedings of the 1st ACM SIGCHI/SIGART conference on Human-robot interaction*, 2006.

[14] K. L. Koay, E. A. Sisbot, D. S. Syrdal, M. L. Walters, K. Dautenhahn, and R. Alami, "Exploratory study of a robot approaching a person in the context of handing over an object.," in *AAAI spring symposium: multidisciplinary collaboration for socially assistive robotics*, 2007.

[15] J. T. Butler and A. Agah, "Psychological effects of behavior patterns of a mobile personal robot," *Autonomous Robots*, 2001.

[16] J. R. Cauchard, J. L. E, K. Y. Zhai, and J. A. Landay, "Drone & me: an exploration into natural human-drone interaction," in *Proceedings of the 2015 ACM International Joint Conference on Pervasive and Ubiquitous Computing - UbiComp '15*.

[17] B. A. Duncan and R. R. Murphy, "Comfortable approach distance with small Unmanned Aerial Vehicles," in *2013 IEEE RO-MAN*.

[18] A. Yeh, P. Ratsamee, K. Kiyokawa, Y. Uranishi, T. Mashita, H. Takemura, M. Fjeld, and M. Obaid, "Exploring proxemics for human-drone interaction," in *Proceedings of the 5th international conference on human agent interaction*, 2017.

[19] W. Jensen, S. Hansen, and H. Knoche, "Knowing You, Seeing Me: Investigating User Preferences in Drone-Human Acknowledgement," in *Proceedings of the 2018 CHI Conference on Human Factors in Computing Systems - CHI '18*, ACM Press.

[20] A. D. Dragan, K. C. Lee, and S. S. Srinivasa, "Legibility and predictability of robot motion," in *2013 8th ACM/IEEE International Conference on Human-Robot Interaction (HRI)*.

[21] A. D. May, C. Dondrup, and M. Hanheide, "Show me your moves! conveying navigation intention of a mobile robot to humans," in *2015 European Conference on Mobile Robots (ECMR)*.

[22] H. Khambhaita, J. Rios-Martinez, and R. Alami, "Head-body motion coordination for human aware robot navigation," in *9th International workshop on Human-Friendlly Robotics (HFR 2016)*, p. 8p, 2016.

[23] J. Hart, R. Mirsky, X. Xiao, and P. Stone, "Incorporating gaze into social navigation," *arXiv e-prints*, pp. arXiv–2107, 2021.

[24] A. Bevins and B. A. Duncan, "Aerial flight paths for communication: How participants perceive and intend to respond to drone movements," in *Proceedings of the 2021 ACM/IEEE International Conference on Human-Robot Interaction*.

[25] T. Kruse, A. Kirsch, H. Khambhaita, and R. Alami, "Evaluating directional cost models in navigation," in *Proceedings of the 2014 ACM/IEEE international conference on Human-robot interaction*.

[26] E. Sisbot, L. Marin-Urias, R. Alami, and T. Simeon, "A Human Aware Mobile Robot Motion Planner," *IEEE Transactions on Robotics*, 2007.

[27] H. Khambhaita and R. Alami, "Viewing robot navigation in human environment as a cooperative activity," in *International Symposium on Robotics Research (ISSR)*, 2017.

[28] P.-T. Singamaneni and R. Alami, "Hateb-2: Reactive planning and decision making in human-robot co-navigation," in *International Conference on Robot & Human Interactive Communication*, 2020.

[29] H.-J. Yoon, C. Widdowson, T. Marinho, R. F. Wang, and N. Hovakimyan, "Socially aware path planning for a flying robot in close proximity of humans," *ACM Transactions on Cyber-Physical Systems*, 2019.

[30] D. Szafir, B. Mutlu, and T. Fong, "Communication of intent in assistive free flyers," in *Proceedings of the 2014 ACM/IEEE international conference on Human-robot interaction - HRI '14*, ACM Press.

[31] S. Chitta, I. Sucan, and S. Cousins, "MoveIt! [ROS Topics]," *IEEE Robotics & Automation Magazine*, 2012.

[32] J. Pan, S. Chitta, and D. Manocha, "FCL: A general purpose library for collision and proximity queries," in *2012 IEEE International Conference on Robotics and Automation*.

[33] D. Sidobre and K. Desormeaux, "Smooth cubic polynomial trajectories for human-robot interactions," *Journal of Intelligent & Robotic Systems*, vol. 95, no. 3, pp. 851–869, 2019.

[34] J. Mainprice, E. A. Sisbot, T. Siméon, and R. Alami, "Planning safe and legible hand-over motions for human-robot interaction," in *IARP/IEEE-RAS/EURON workshop on technical challenges for dependable robots in human environments*, 2010.

[35] E. A. Sisbot and R. Alami, "A human-aware manipulation planner," *IEEE Transactions on Robotics*, 2012.